Harshita

Provisioning radio fallback for directional wireless channels

Master's Thesis in Computer Engineering

28 September 2020

Provisioning radio fallback for directional wireless channels

Master's Thesis in Computer Engineering

vorgelegt von

Harshita

geb. am 03 October 1994
in Lucknow, India

angefertigt in der Fachgruppe

Distributed Embedded Systems
(CCS Labs)

Heinz Nixdorf Institut
Universität Paderborn

Betreuer:	**Max Schettler**
	Muhammad Sohaib Amjad
Gutachter:	**Falko Dressler**
	Christian Scheideler
Abgabe der Arbeit:	**28. September 2020**

Erklärung

Ich versichere, dass ich die Arbeit ohne fremde Hilfe und ohne Benutzung anderer als der angegebenen Quellen angefertigt habe und dass die Arbeit in gleicher oder ähnlicher Form noch keiner anderen Prüfungsbehörde vorgelegen hat und von dieser als Teil einer Prüfungsleistung angenommen wurde.

Alle Ausführungen, die wörtlich oder sinngemäß übernommen wurden, sind als solche gekennzeichnet.

Declaration

I declare that the work is entirely my own and was produced with no assistance from third parties.

I certify that the work has not been submitted in the same or any similar form for assessment to any other examining body and all references, direct and indirect, are indicated as such and have been cited accordingly.

Harshita
(Harshita)
Paderborn, 28 September 2020

Abstract

Wireless technologies have been traditionally challenged to provide sufficient data rates. A promising approach to overcome the challenge is to use novel frequency bands like 28 GHz or 60 GHz (Millimeter Wave (mmWave)) or use Visible Light for Communication (VLC). The mmWave frequency bands provide ample bandwidth to realise high data rates but they also have a significant downside. Line of Sight (LOS) is required between the transmitter and the receiver for propagation. Even small rotations of a device can lead to dramatic changes in the transmission quality. One approach to solving these problems is to have a radio fallback for the directional channels. This can be done by switching to microwave frequency bands in case of obstructions in the LOS path.

In this thesis, an algorithm is proposed for successful determination of LOS link and for switching to microwave frequency in case of blockage. A further improvement of the proposed algorithm using channel estimation is also analysed. Based on the simulations, the results indicate that the fault-tolerant mmWave is better in terms of throughput as compared to normal mmWave. Fault-tolerant mmWave also has lower latencies as compared to normal mmWave.

Kurzfassung

Drahtlose Technologien sind traditionell gefordert, ausreichende Datenraten bereitzustellen. Ein vielversprechender Ansatz zur Bewältigung dieser Herausforderung besteht darin, neuartige Frequenzbänder wie 28 GHz oder 60 GHz (mmWave) oder VLC zu verwenden. Die mmWave -Frequenzbänder bieten eine ausreichende Bandbreite, um hohe Datenraten zu erzielen, haben jedoch auch einen erheblichen Nachteil. Für die Weitergabe ist zwischen Sender und Empfänger LOS erforderlich. Selbst kleine drehungen eines Geräts können zu dramatischen Änderungen der Übertragungsqualität führen. Ein Ansatz zur Lösung dieser Probleme besteht darin, einen Funk-Fallback für die Richtungskanäle zu haben. Dies kann durch Umschalten auf Mikrowellenfrequenzbänder bei Hindernissen im LOS geschehen.

In dieser Arbeit wurde ein Algorithmus zur erfolgreichen Bestimmung der LOS -Verbindung und zum Umschalten auf Mikrowellenfrequenz im Falle einer Blockierung vorgeschlagen. Eine weitere Verbesserung des vorgeschlagenen Algorithmus unter Verwendung der Kanalschätzung wird ebenfalls analysiert. Basierend auf den Simulationen zeigen die Ergebnisse, dass die fehlertolerante mmWave hinsichtlich Durchsatz und Latenz besser ist als die normale mmWave.

Contents

Chapter 1

Introduction

The increase in the amount of mobile data traffic and the emergence of various applications like mobile internet, virtual reality etc., has led to the demand for more bandwidth and higher data rates of wireless networks [1]. Exploiting the enormous spectrum of the Millimeter Wave (mmWave) bands can greatly increase the communication capacities [2]. One of the main advantages of the mmWave is the broader spectrum available for communication. This can be put to use when shifting from 4G communication to 5G as broader spectrum can provide higher data rates [3]. The millimeter wave frequencies can provide fronthaul and backhaul wireless transport in radio access network architecture [4]. Millimeter wave devices enable large antenna arrays to be packed in small dimensions owing to short wavelengths. This can improve signal directivity by reducing co-channel interference and enhance link reliability. Having large number of small antennas also enables the employment of Multiple Input Multiple Output (MIMO) techniques, multiplexing, diversity and beamforming [5]. The effect of diffraction decreases with an increase in frequency because objects such as buildings introduce sharp shadows [6].

Meanwhile, mmWave communications have few disadvantages [5].The major disadvantages of mmWave are blockage and deafness. The high signal attenuation of mmWave due to its inability to propagate through common objects is termed as blockage [3]. For example, millimeter waves incur a loss of 20-35 dB due to the human body and 20-30 dB due to furniture in the environment [7]. Compared to lower frequencies, millimeter waves are more vulnerable to atmospheric attenuation and human shadowing [2]. Millimeter waves are also highly directional [8]. The misalignment between the main antenna beams of transmitter and receiver causes high signal attenuation which is known as deafness [7]. This affects the network capacity and reliability.

Hence, there is a need to look for fault-tolerant approaches to reduce the effects of all extreme attenuations. One method to avoid attenuation due to blockage is to

use a relaying technique in which the source node uses an intermediate node (called relay) to bypass the obstacles [9]. However, the source-relay and relay-destination pairs take time to setup and also have to undergo beam training.

Another method is to switch to conventional microwave frequencies when the obstacle appears and later return to mmWave bands. Lower frequencies can more easily penetrate through objects thereby eliminating loss due to blockage. Microwave frequencies are typically less directional hence the need for beam alignment is reduced. Shadow fading and doppler spread increases with frequency [6]. Hence lower frequencies have an advantage of less shadow fading and doppler spread. For scenarios with high mobility which require frequent beam training procedures, switching to microwave frequencies is delay optimal [9]. The above mentioned points indicate that using microwave frequencies as a fallback for mmWave link has an advantage over other methods.

The main goal of this thesis is to specify the requirements of a radio fallback system spanning across directional and non-directional wireless channels. I have devised a mechanism for successful determination of the presence of Line of Sight (LOS) link and for switching to microwave frequency in case of blockage. I have done a comparison study of two types of models of this switching mechanism. To extend this algorithm to multiple nodes, I have used this algorithm along with the channel estimation technique. In order to examine the performance of the algorithm, I collect data from the simulations and compare the different approaches on the basis of different metrics.

Chapter 2

Related Work

In recent years, the research community has been focusing on mmWave frequency for communication because of various advantages [5]. Various studies like [5], [8], [2] etc. related to mmWave frequency have been done which provide an insight about the advantages, challenges, channel models, opportunities etc. A major challenge with mmWave is the loss of signal due to blockage in LOS path.

One method to avoid attenuation due to blockage is to use a relaying technique in which the source node uses an intermediate node (called relay) to bypass the obstacles [9]. Congiu et al. [9] considers a source node, a destination node and a relay node. The communication link is established between the source and destination node with mmWave frequency bands in case of no blockage or by the relay node in case of obstruction in the LOS path. However, the source-relay and relay-destination pairs take time to setup and also have to undergo beam training.

Kong et al. [10] propose a novel method, which they termed as AutoRelay, for mmWave communication using unmanned autonomous vehicles such as drones and self-driving cars as mobile relays. In the paper [11] the authors investigate the potential benefits of the relay aided mmWave networks. The performance in terms of Signal-to-Noise Ratio (SNR) improves but the complexity of the network is increased.

Another method is to switch to conventional microwave frequencies when the obstacle appears and later return to mmWave bands to take advantage of the wide spectrum offered by mmWaves and avoid losses due to blockages in the LOS path. Authors in [12], propose such hybrid communication networks in Device-to-Device (D2D). They have designed an improved beam alignment protocol among base stations and D2D equipment which helps to select between microwave mode and millimeter wave mode. The hybrid D2D communication mode outperforms both the normal mmWave and microwave mode in terms of area spectral efficiency and coverage probability. I have designed a switching algorithm as opposed to beam

alignment protocol designed in [12]. The protocol is based on probability rather than actual detection of blockages which is implemented in this thesis.

Semiari et al. [13] introduces the first comprehensive tutorial for integrated mmWave-microwave communications. It discusses the key concepts like architectures for radio interface, resource allocation methods along with mobility management. An integrated mmWave-microwave wireless network has been proposed which can reap the benefit of multi-RAT (radio access technology) capability. It is also capable of dealing with the intermittent nature of mmWave links. The proposed wireless network would lead to the higher complexity of MAC protocols.

In another study, relay and fallback methods of the mmWave communications have been compared based on throughput and delay. Congiu et al. [9] states that for scenarios with high mobility which require frequent beam training procedures, switching to microwave frequencies is delay optimal. The relay option is better when there is heavy traffic and the communication needs higher bandwidth of mmWave.

Switching to microwave frequencies can be done more efficiently based on the mmWave channel estimation or by detecting blockages using microwave frequencies. Deep learning models have been used in [14], [15] for detecting LOS and channel estimation respectively. Alrabeiah and Alkhateeb in [14], have proven that a sufficiently large neural network can learn mapping functions that predict blockage status of mmWave analytically using sub-6 GHz frequency. In [16], the authors have proposed a two-stage channel estimation scheme for mmWave MIMO. Using sparse Bayesian learning they have obtained a coarse channel estimate and refined it using maximum likelihood estimator. The proposed estimator can almost achieve the upper bound of Cramér-Rao Bound.

Implementation of various fallback and relay methods need various channel models and blockage models for simulation of real life environments. Different publications have analysed the performance of millimeter wave communications using various channel models [17], [18], [19]. Various studies propose different kinds of blockage models which have been used for mmWave networks. In [20], the author proposes a statistical blockage model, using experimental mmWave channel measurements, which accounts for random appearance and disappearance of the blockages. Another publication [21] proposes a model which addresses an angular correlation between the obstacles in the communication link. The models proposed in both [20] and [21] have been used for network throughput analysis and lack delay analysis of a mmWave network.

Chapter 3

Fundamentals

In this chapter, I will introduce the concepts which form the basis of this thesis. First, I will explain millimeter waves, their advantages, disadvantages and applications. In Sections 3.2 and 3.3, I will detail the different types of path losses, channel model and channel estimation techniques.

3.1   Millimeter Wave

The mmWave band roughly correspond to 30 GHz to 300 GHz. This huge unlicensed bandwidth available has attracted large research interest. Currently, the available bandwidth for mobile networks (2G, 3G, 4G and LTE-Advanced spectrum) is globally smaller than 780 MHz and each major wireless provider has only a total of about 200 MHz spectrum [3]. This bandwidth is not sufficient for providing rates of Gbit/s to multiple devices since a huge per-device spectral efficiency would be required. However, in mmWave bands, there are large chunks of bandwidth available for future mobile networks. mmWave communication systems that can achieve multigigabit data rates at a distance of up to a few kilometres already exist for point-to-point communication [22].

Pi and Khan have described the different uses of the 3-300 GHz spectrum as shown in Figure 3.1. 300 MHz-3 GHz is used for commercial wireless communications because of its favorable propagation characteristics. Approximately, 252 GHz (denoted in Figure 3.1 is available within 3-300 GHz range for mobile broadband. The frequencies in the range of 57-64 GHz can experience an attenuation of upto 15 dB/km with maximum attenuation due to oxygen absorption at around 60 GHz. Unlicensed use of the ultra-wideband from 3.1-10.6 GHz frequencies has been proposed for enabling high data rates in personal area networks.

Millimeter wave devices enable large antenna arrays to be packed in small dimensions owing to short wavelengths. This can improve signal directivity by
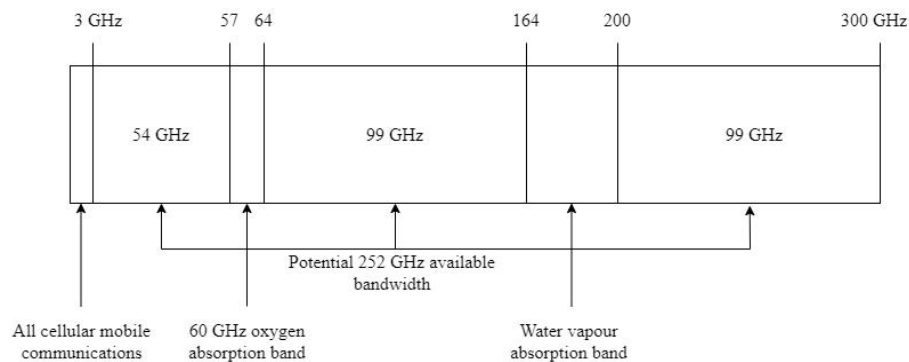
Figure 3.1 – Millimeter wave spectrum [22]

reducing co-channel interference and enhance link reliability. Large arrays may enable precoding multiple data streams which could improve spectral efficiency [23]. The security is also increased since the signal is limited to a small area. The components and antennas of mmWaves are usually very small hence it is possible to make lightweight equipment. The effect of diffraction decreases with an increase in frequency because objects such as buildings introduce sharp shadows [6].

Meanwhile, mmWave communications have few disadvantages [5]. The major disadvantages of mmWave are blockage and deafness. The high signal attenuation of mmWave due to its inability to propagate through common objects is termed as blockage [3]. Compared to lower frequencies, mmWaves are more vulnerable to atmospheric attenuation, human shadowing [2] and are also highly directional [8]. The misalignment between the main antenna beams of transmitter and receiver causes high signal attenuation which is known as deafness [7]. This affects the network capacity. Due to the small size of the antennas, the cost of manufacturing hardware of such great precision increases. Moreover, sharing such links between multiple devices comes with a higher overhead as compared to non-directional technologies [24].

mmWave technology can be readily used for stationary short distance scenarios. It becomes difficult to handle the mobility of the transmitter or the receiver because of the high directionality of the antennas and the limited range of communication [25].

3.1.1 Applications

Millimeter waves with frequencies in the license range 71-76, 81-86 and 92 to 95 GHz are usually used for the high bandwidth, point-to-point communication links while the 60 GHz frequency is used for the unlicensed short-range data links

such as the Wireless Gigabit (WiGig), based on the standard 802.11ad protocol. mmWaves are used in communications, imaging, astronomy, medicine [26] etc. Large bandwidth makes mmWave favourable for transmission of High Definition (HD) videos. A mmWave system is proposed to provide HD videos up to 3 Gbs Multimedia QoS characterization was modelled by critical measurements and designed a QoS aware multimedia scheduling scheme to succeed the complexity with the optimum performance [27].

Wireless Gigabit (WiGig) technology enables devices to communicate at high data rates of up to 7 or 8 Gb/sec. The millimeter radars in the 76 to 81 GHz range are widely used in vehicle control and safety devices. The specific applications include sensors for automatic braking, lane intrusion, applications blind spot detection, forward collision detection, cruise control, and more.

mmWave communications are used in vehicular networks, virtual reality, satellite communications and 5G. Active and passive imaging systems have been developed in the range from 30-300 GHz. They can penetrate through poor weather conditions and also see through materials such as cloth, polymers etc. [28].

Apart from being used in communications, mmWaves are used for imaging, tracking and detecting. For example, mmWaves can be used to explosive detection on personnel since the waves can pass through clothing and are easily reflected by human bodies and concealed objects [29]. These reflected wavefronts can be used for imaging the shape and size of the object.

3.2   Path Loss

The data transmitted through any channel is bound to have a few losses. Any channel can experience losses such as Free Space Path Loss (FSPL), atmospheric attenuations, fading, shadowing, thermal noise etc.

3.2.1   Free Space Path Loss

The signal transmitted from the transmitted travels as a light wave in a spherical shape with the transmitter as the centre of the sphere. The receiver receives power from a particular cross-section area of the sphere. The power per unit cross-section area decreases as the distance between the transmitter and receiver increases. This loss is expressed by the free space path loss formula which is derived from the Friis Transmission formula

$$FSPL = \left(\frac{4\pi d}{\lambda} \right)^2 \qquad (3.1)$$

The loss is directly proportional to the distance between the transmitter and receiver d and inversely proportional to the wavelength of the signal λ. The FSPL increases with frequency and distance.

3.2.2 Atmospheric Attenuation

The FSPL describes only the part of attenuation which occurs when the signal travels in vacuum. However, in reality, the signals do not travel vacuum; they interact with air and other particles and tend to lose their energy while travelling since the molecules absorb the energy from the signal. The attenuation varies with factors like temperature, pressure, etc. In the Earth's atmosphere, the two major absorbing gases at mmWave frequencies are oxygen (O_2) and water (H_2O). The sea level at zero-meter altitude is the worst-case scenario for atmospheric attenuation, since at zero-altitude the air density reaches its maximum, while at higher altitudes the air density decreases, which culminates a reduced attenuation. This implies that attenuation is directly proportional to the density.
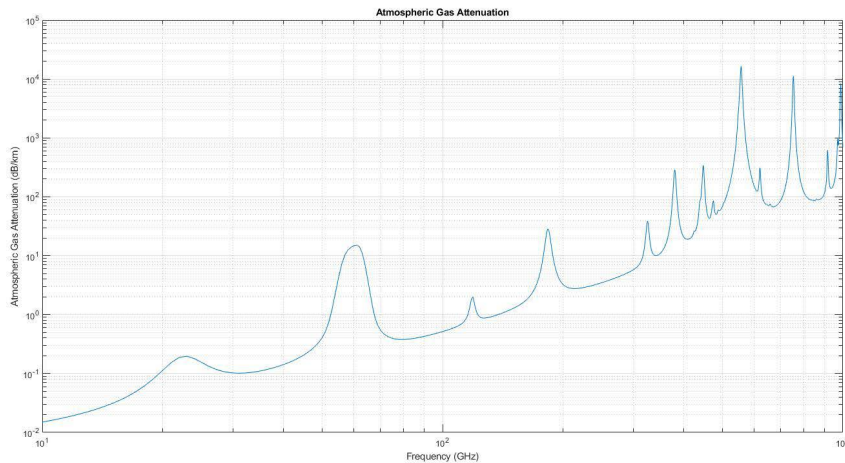
Figure 3.2 – Average atmospheric attenuation of millimeter waves [30]

The atmospheric attenuation due to absorption by O_2 is strongest at 60 GHz as can be seen in Figure 3.2 due to an absorption band created by the broadened and overlap of the spectral lines of oxygen from the atmospheric pressure near the ground [30]. The attenuation due to oxygen can reach values in the range of 15 dB/km, yet it is important to mention that the intensity of attenuation is a function of various factors like temperature, pressure etc.

3.2.3 Shadowing

The mmWave frequencies do not propagate well through obstacles, such as furniture, doors, walls and other paraphernalia [22]. Such obstacles can cause variations in the signal which is known as shadowing or shadow fading. The three basic propagation mechanisms which are affected by the obstacles present in the environment are reflection, diffraction and scattering. The transmission scenario can provide information about the shadowing component in the environment. The small wavelength of the mmWaves makes it prone to scattering.

Reflection occurs when the signal impinges upon an object which has very large dimensions when compared to the wavelength of the propagating signal. Reflection occurs from the surface of the earth, buildings and walls.

Diffraction occurs when the path between the transmitter and the receiver has objects with sharp edges or irregularities. At higher frequencies, diffraction depends on the geometry of the object as well as the amplitude, polarization and phase of the incident wave at the point of diffraction.

Scattering is a general physical process where the signal deviates from the straight trajectory by one or more paths. It occurs when the environment has objects which are smaller than the wavelength of the signal being transmitted. Scattered waves are produced by rough surfaces and small objects.

3.2.4 Fading

In wireless communications, fading is the deviation of the power of the electromagnetic signal from the average value caused by obstacles which affect wave propagation. Figure 3.3 gives a classification of the various types of fading in wireless communication channels. There are two different types of fading: large scale fading and small scale fading. Small scale fading is caused by interference between two or more waves of the transmitted signal which arrive at the receiver at slightly different times. These waves, called multipath waves, interfere at the receiver to give the resultant received signal. Small scale fading is often handled with diversity schemes. Large scale fading is dependent on the location concerning obstacles. It is affected by prominent terrain contours like mountains, forests, buildings etc. between the transmitter and the receiver [31]. The statistics of large scale fading provide a way of computing path loss as a function of distance.

Small scale fading can be divided into two types: multipath delay spread and doppler spread. Multipath delay spread is the difference in arrival between the first component and the latest multipath component. Doppler spread is the widening of the spectrum of a narrowband signal due to the relative motion between the transmitter and the receiver [31]. Large scale fading can also be divided into two types: path loss and shadowing. These have been discussed in Section 3.2.
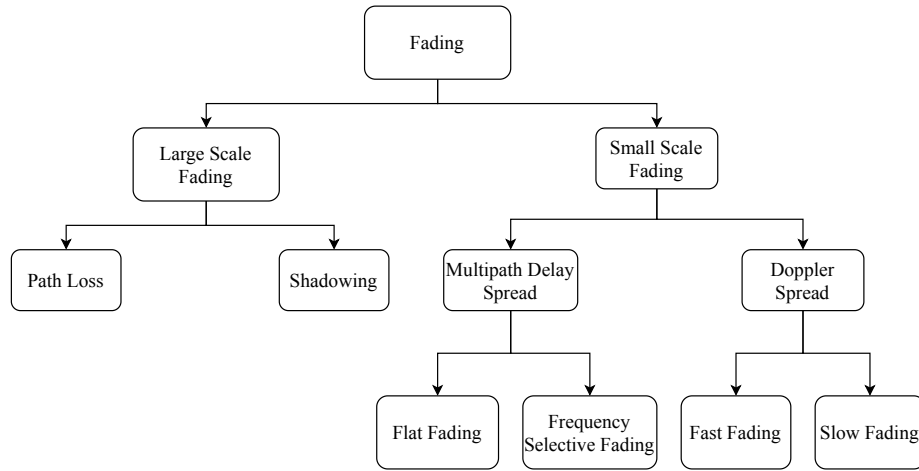
Figure 3.3 – Types of fading in wireless communication channels

Fast fading refers to the swift fluctuations in the amplitude, phase or multipath delays of the received signal, due to the interference between the multiple versions of the same transmitted signal arriving at the receiver at a slightly different time interval. Slow fading occurs when objects that partially absorb the energy of the transmission signal between the transmitter and the receiver. In this thesis, slow fading is considered, i.e. the channel coherence time exceeds the observation time.

3.3 Channel Model

Before the actual implementation of hybrid communication or fallback mechanism for mmWave, it is necessary to study the propagation characteristics of mmWave using channel models. There are numerous works available on millimeter wave channel models. For example, [32] introduces a quasi-deterministic channel model with a focus on millimeter wave outdoor access channels. The authors of [33] propose a channel model based on 3rd Generation Partnership Project (3GPP) spatial channel model framework. This model meets the requirements of beam-tracking evaluation while keeping spatial consistency. There are also other physical channel models like two ray fading model [34], Saleh Valenzuela model [35] which are based on the physical channel parameters like path loss, fading etc.

A channel model is an important piece of physical layer communication simulation. It is the radio propagation model which determines the characteristics of any communication system. The channel model can be the impulse response of the channel in the time domain or its Fourier transform in the frequency domain.

Channel models are generally classified into two categories as shown in Figure 3.4. A physical channel model is constructed based on the electromagnetic characteristics
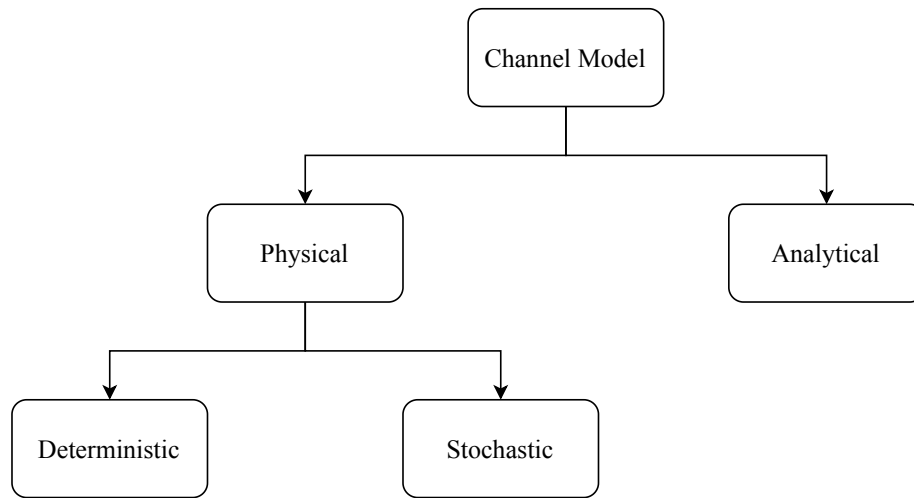
Figure 3.4 – Channel model classification [5]

of the signal propagating between the transmit and receive antenna arrays, while an analytical channel model is described based on the mathematical analysis of the channel [5].

A physical channel model is further classified as deterministic and stochastic model. The deterministic channel model is recognized to be very accurate in predicting channel characteristics but have high computation and modelling complexity [5]. Such models are used when the propagation environment is known. On the other hand, the stochastic channel models are based on measurements done in different scenarios. Probability Density Function (PDF) is used to represent channel parameters and then fading components are calculated. These are not environment specific [5].

3.4 Channel Estimation

As described in Section 3.2, the signal undergoes attenuation when passing through a channel. The received signal can be decoded properly without much errors by removing the distortions added by the channel. This can be done when the characteristics of the channel are known. The process/technique to characterize the channel is called channel estimation. Channel estimation can be carried out in different ways: with or without the help of a parametric model, using frequency and/or time correlation properties in the wireless channel, blind methods or those based on training pilots, adaptive or non-adaptive methods. There are mainly two types of channel estimators: Least Square (LS) and Minimum Mean-Square Error (MMSE). The LS or Linear Minimum Mean-Square Error (LMMSE) is used as a reference

model [36]. The LS estimation is the simplest channel estimation based on parallel Gaussian channel model in frequency domain. LS does not use any prior information so the performance is worse than LMMSE whereas the LMMSE uses the channel covariance matrix and SNR for better performance [37].

Discrete Fourier Transform (DFT) based channel estimation technique can be used to further improve the performance of LS and MMSE estimators by eliminating the effect of noise outside the maximum channel delay [38]. Mathematically, this can be described using Equations 3.2 and 3.3 [38].

$$IDFT\{\hat{H}[k]\} = h(n) + z(n) \triangleq \hat{h}[n], \; n = 0, 1...., N-1 \tag{3.2}$$

where $\hat{H}[k]$ is the channel estimate and $z[n]$ denotes the noise component in time domain. Ignoring the coefficients of $\hat{h}[n]$ that contain noise only, the equation can be rewritten as:

$$\hat{h}_{\text{DFT}}[n] = \begin{cases} h[n] + z[n] & n = 0, 1, ..., L-1 \\ 0 & \text{otherwise} \end{cases} \tag{3.3}$$

where L is the maximum channel delay. The remaining L elements are transformed back to frequency domain.

$$\hat{H}_{\text{DFT}}[k] = DFT\{\hat{h}_{\text{DFT}}(n)\} \tag{3.4}$$

Orthogonal Frequency Division Multiplexing (OFDM), a type of multi-carrier system, can be used along with channel estimation for better data rates and higher spectral efficiencies. Each subcarrier in OFDM can be regarded as an independent channel (as long as no inter-channel interference occurs). The orthogonality allows each subcarrier component of the received signal to be expressed as the product of the transmitted signal and channel frequency response at the subcarrier. Thus, the transmitted signal can be recovered by estimating the channel response just at each subcarrier. In general, the channel can be estimated by using pilot symbols known to both transmitter and receiver, which employ various interpolation techniques (e.g., linear or spline interpolation) to estimate the channel response of the subcarriers between pilot tones [38].

Chapter 4

Methodology

Based on the concepts explained in Chapter 3, I will explain how the system has been implemented in MATLAB and reasons for using the particular components in the system. I will also describe the fallback mechanism implemented and the blockage model considered in the implementation.

4.1   System Model

In this implementation, a deterministic channel model is used with constant attenuation at a distance of 1 m and distance-dependent attenuation. A constant loss due to any obstacle in the path is also considered. The channel model which I have implemented is a fading channel with Additive White Gaussian Noise (AWGN). I have considered a Rician fading channel with three discrete paths. A Single Input Single Output (SISO) system is implemented initially. A high level diagram of the system model is shown in Figure 4.1. The implemented model consists of Quadrature Phase Shift Keying (QPSK) modulator and Root Raised Cosine (RRC) transmit filter on the transmitter side and QPSK demodulator and RRC receive filter on the receiver end.
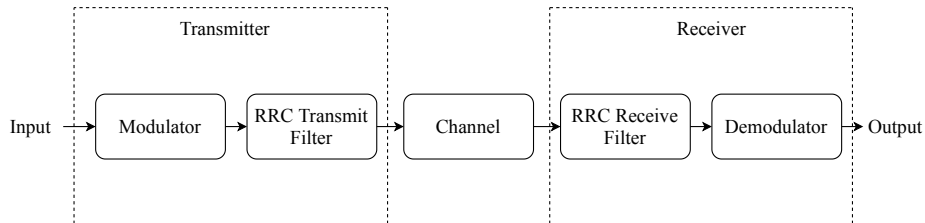
Figure 4.1 – System Model which shows the transmitter consisting of the modulator and the RRC transmit filter. The channel is a Rician fading channel. On the receiver side, the two blocks are the RRC receive filter and the demodulator.

In wireless communications, there are two conflicting requirements: demand for higher data rates and narrower bandwidth (more users, more channels and less noise). If the channels are too narrow, at sampling points in time there will be an overlap of symbols. One possible solution to this is the use of an ideal low pass filter. An implementation of the low-pass Nyquist filter is RRC filter. It is used for pulse-shaping and minimising the effect of jitter. The filter is split into two parts to further improve the noise cancellation.

$$H_{rc}(\omega) = H_{rrc,tx}(\omega)H_{rrc,rx}(\omega) \tag{4.1}$$

RRC filter equation in frequency domain is given by

$$H(f) = \begin{cases} 1 & |f| \le \frac{1-\beta}{2T} \\ \frac{1}{2}\left[1 + \cos\left(\frac{\pi T}{\beta}\left[|f| - \frac{1-\beta}{2T}\right]\right)\right] & \frac{1-\beta}{2T} \le |f| \le \frac{1+\beta}{2T} \\ 0 & \text{otherwise} \end{cases} \tag{4.2}$$

The baseband signals are incompatible for direct transmissions hence there is a need for modulation. The various modulation schemes were simulated for the current implementation considering Rician fading. The Bit Error Rate (BER) vs SNR graph for each modulation scheme was plotted along with the theoretical values. As seen in Figure 4.2, QPSK modulation has the lowest BER as compared to other modulation schemes. Binary Phase Shift Keying (BPSK) has comparable BER values for SNR values (Eb/No) but the bandwidth of QPSK is twice as efficient as BPSK. Hence, QPSK modulation is used in the final implementation.
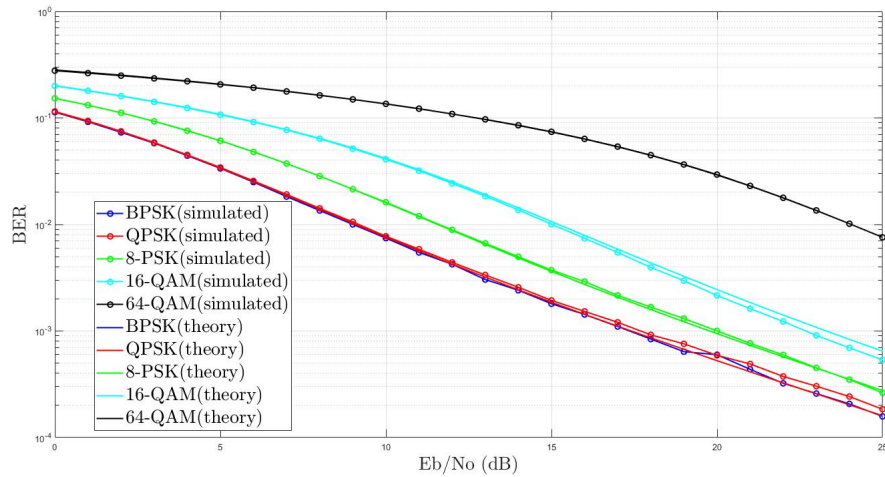
Figure 4.2 – Comparison of modulation schemes for Rician fading channel with AWGN

The channel consists of a blockage model, a multipath fading channel and an AWGN channel. In the next two Subsections 4.1.1 and 4.1.2, I have described the fallback mechanism and the blockage model in detail.

Further improvements in the radio fallback mechanism of the mmWave can be done using channel estimation techniques. The system implemented for channel estimation is a MIMO OFDM system having two transmit and two receive antennas. A high level block diagram of the MIMO OFDM system is shown in Figure 4.3.
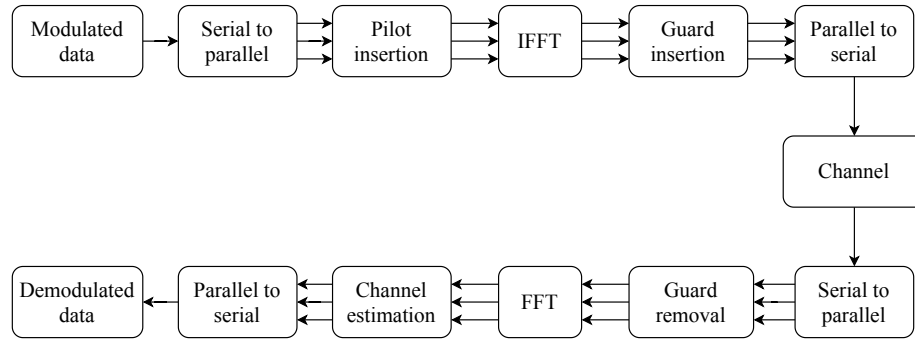
Figure 4.3 – High level block diagram of MIMO OFDM system [39]

In an OFDM system, the modulated data is converted to parallel data streams. Pilot symbols are inserted. This data along with pilot symbols undergoes Inverse Fast Fourier Transform (IFFT) to convert them into time-domain signals. Guard symbols are inserted after IFFT to reduce Inter Symbol Interference (ISI). The parallel signals are converted to serial again before transmitting it through the channel. On the receiver side, the serial data is again converted to parallel. The guard symbols are removed and a Fast Fourier Transform (FFT) is performed. Channel estimation is done and before demodulation, the parallel data is converted back to serial data.

I have used this OFDM MIMO system for extending the system to multiple nodes. Channel estimation technique is used to determine the state of links between the transmitter and the receiver. A system having one transmitter and five receivers is implemented. It is possible to have LOS in other receivers in case it is blocked for one (as shown in Figure 4.4).

The links between the transmitter and each receiver are treated as a separate channels having same channel characteristics. Channel estimation is performed for each link to check for the presence of direct communication link. This helps in reducing the latency as the LOS check is not done before transmitting each packet as in the case of single transmitter and single receiver.
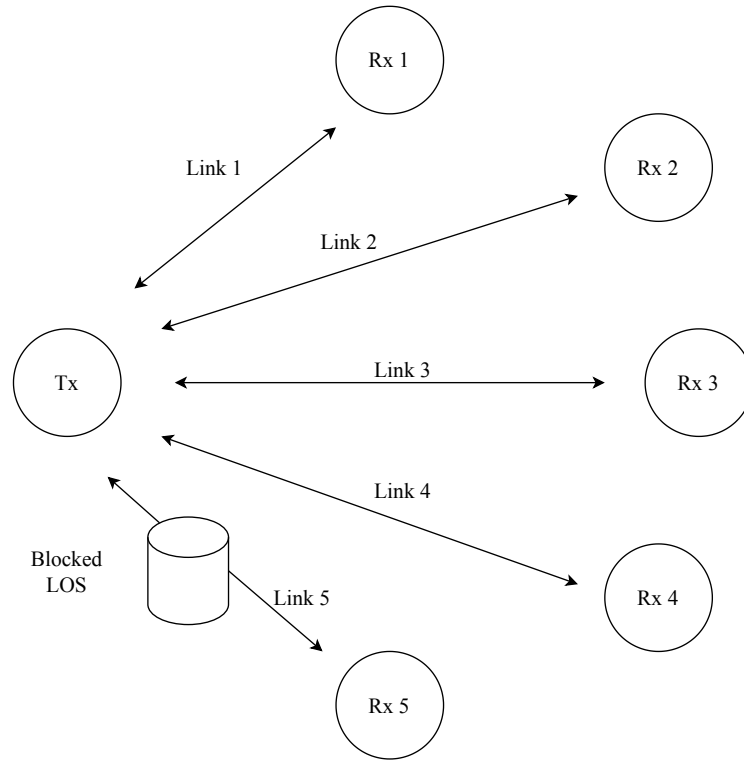
Figure 4.4 – System model with single transmitter and five receivers. It is possible to have LOS between other links when one the link is blocked. An example of the same is depicted.

4.1.1 Blockage Model

It is difficult to model mobility of blockages in MATLAB. Hence, an abstraction of the blockages is used [9]. The channel is modelled as a queue system where the presence of a message in the queue denotes obstruction in the direct path whereas an empty queue implies availability of LOS path. The messages do not refer to the real messages but only to the blockage occurrences. The busy period of the server is the time for which the direct path between the transmitter and receiver is blocked. The blockage model adds randomness to the appearance and disappearance of the obstruction in the communication link. The maximum queue length has been fixed to 10 i.e., more than 10 obstacles are not possible in the direct path between the transmitter and receiver. The arrival and departure rates follow a Poisson distribution. This can be easily extended to other types of distributions. There is no time correlation between the appearance and disappearance of the obstacles in the communication link.

4.1.2 Fallback Mechanism

There are two fallback mechanisms implemented in this thesis. The first mechanism is used for single transmitter and receiver and the second mechanism is used for multiple nodes. The first mechanism uses a switching algorithm to check for the presence of LOS path between the transmitter and the receiver. It is a two-step check which is done before transmitting each packet. The first step is to send a test signal in the millimeter range frequency to the receiver. The received power is measured and compared with the fixed threshold ($P_{threshold}$). If the power received exceeds the $P_{threshold}$ then the second check is done. In case of power received being less than the $P_{threshold}$, the packet is transmitted using microwave frequency. Figure 4.5 shows a flowchart with the different steps of the algorithm.
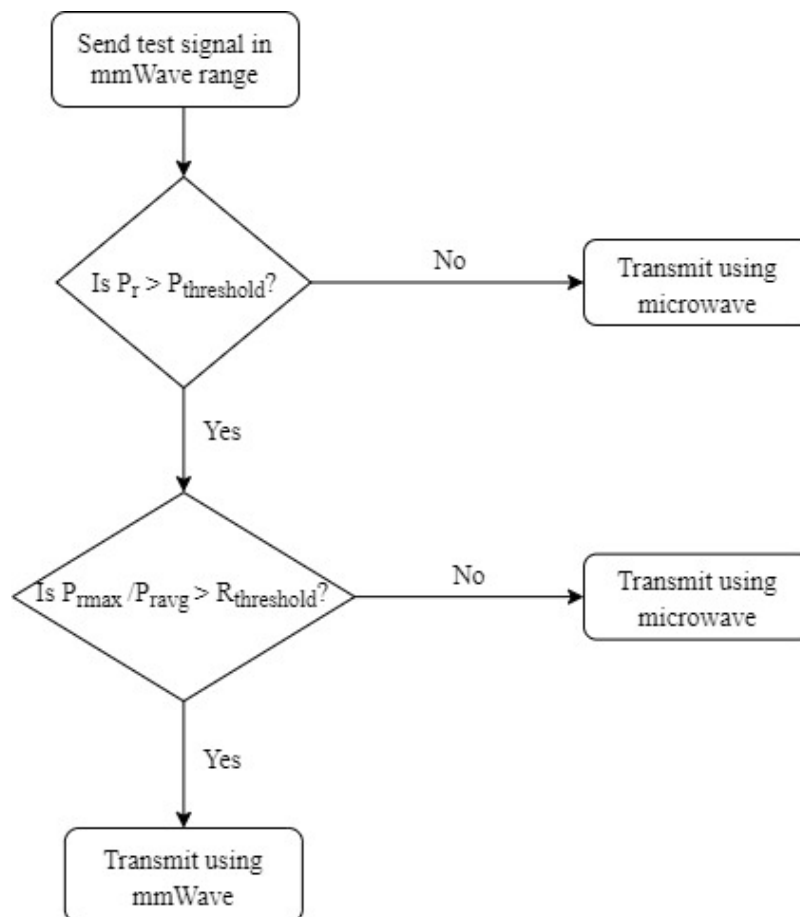
Figure 4.5 – Algorithm used for switching between frequencies when an obstacle is present in the LOS path between the transmitter and the receiver

For the second check, the ratio of highest signal strength component to average received signal energy is measured. This ratio is also compared to a fixed threshold ($R_{threshold}$). If the ratio is greater than the $R_{threshold}$, the packet is transmitted using mmWave frequency else microwave frequency is used. This ratio of highest signal strength to average received signal energy is used because strong multipath spreads the incidence energy over a wide range of the angular receive profile and thus increases the denominator of the fraction. A direct path on the other hand results in a sharp peak at its incidence angle and increases the ratio. As the direct path peak loses magnitude by the blockage, the numerator of the ratio shrinks while the average energy received through reflections remains. The time taken to complete the check for LOS presence is of the order of 10^{-7} seconds and the channel is assumed constant during this small time. Hence, the channel state information is not outdated.

An assumption is made that the mmWave has only two states LOS and non Line of Sight (nLOS). It is also assumed that there are zero outages in the microwave link. Each obstacle in the communication link increases the attenuation of the signal. As the number of obstacles increases, the signal attenuation increases. Shadowing and fading (as explained in Subsections 3.2.3 and 3.2.4) are the major reasons for the attenuations due to obstacles.

The second fallback mechanism uses channel estimation technique to detect the presence of blockage between the transmitter and the receiver. A system with multiple receiver nodes is considered. Instead of using the switching algorithm for checking the presence of LOS between each receiver and transmitter, the transmitter determines the state of the links by employing MIMO OFDM channel estimation. Obstacle locations are constant during channel estimation and data transmission interval. To initiate the channel estimation process, the transmitter sends training beams to one of the receivers. These beams are utilised by the receiver to estimate the channel. In case of blockage, the power will be reduced. This power will be compared to the theoretical channel to deduce the difference. In case of reduced power, the receiver sends back a message indicating the need to switch to microwave frequency. In the other case (when there is no blockage), the receiver sends an acknowledgement indicating that mmWave frequency can be used for transmission.

Chapter 5

Evaluation

This chapter provides the implementation details and the analysis of the fallback mechanism implemented. I also describe the results I obtained and the effects observed.

5.1 Simulation Setup

In order to evaluate the performance of the fallback mechanisms, I observe their behaviour in simulations. A simple simulation scenario is designed which can be applied to fault-tolerant mmWave as well as microwave link and simple mmWave link. The simulations have been run in Matlab2020a.

For the first setup, two SISO nodes are considered: one of them is a transmitter and the other is a receiver. The distance between the transmitter and the receiver varies from 10 m to 100 m with intervals of 10 m each. Both the transmitter and the receiver are considered to be stationary at all times contributing to the doppler shift being zero. As stated in [40] loss due to atmospheric attenuations can account for 7-15.5 dB/km power loss. Hence, an indoor scenario has been considered assuming constant atmospheric attenuation. An array of uniformly distributed pseudorandom integers is used as input to the system. A total of 1000 packets are transmitted for each simulation run. The number of repetitions is fixed to 100 for each simulation run because it gives a 95% confidence interval on the metrics recorded. I have used 73 GHz frequency for mmWave communication and a frequency of 2.9 GHz for microwave communication.

After fixing the scenario, the next important step is to have a channel model based on Section 3.3. I have used the built-in functions of Communications Toolbox of Matlab for Rician fading channel. The specifications for the Rician channel have been described in Table 5.1. The Rician K-factor is set as 3 which implies that the first

discrete path is Rician fading process and the other two are independent Rayleigh fading processes.

The blockage model is implemented using M|M|∞ multi-server queuing model. This ensures that there is no correlation between the obstacles. Along with the multipath fading and blockage model, AWGN is also considered for the channel. For the channel, the received signal (in complex baseband form) can be written as

$$y(t) = h(t) * x(t) + n(t) \tag{5.1}$$

where,

- y(t) is the received signal

- h(t) is the channel impulse response

- x(t) is the transmitted signal

- n(t) is the noise (AWGN)

The convolution is given by the integral in Equation 5.2

$$y(t) = \int_{-\infty}^{\infty} x(\tau)h(t-\tau)d\tau + n(\tau) \tag{5.2}$$

where τ is the propagation delay. h(t) is replaced by the impulse responses of the multipath fading channels. These impulse responses can be derived from the probability density functions. The PDF of Rician channel is given by Equation 5.3 [41]

$$pdf(r) = r\frac{r}{\sigma^2}e^{\frac{r^2+A^2}{2\sigma^2}}I_0\left(\frac{r\cdot A}{\sigma^2}\right), \ r \geq 0 \tag{5.3}$$

A denotes the peak amplitude of the dominant signal, r denotes the amplitude of the received signal envelope, σ is the root mean square (rms) value of the received signal voltage. $I_0(*)$ is the modified Bessel function of the first kind and zero-order. K which is called the Rician factor is given by

$$K[dB] = 10 \cdot \log\left(\frac{A^2}{2\sigma^2}\right) \tag{5.4}$$

Parameters	Values
Sample Rate	1×10^5
Path Delays	1×10^{-9} to 1×10^{-6}
Average Path Gains	-20 to 0
K-factor	3

Table 5.1 – Specifications of Rician Fading Channel

If there is no LOS, implies *A* is zero. Equating *A* to zero in Equation 5.3, Equation 5.5 is obtained which is the PDF of Rayleigh fading channel.

$$pdf(r) = \frac{r}{\sigma^2} e^{\frac{r^2}{2\sigma^2}}, \ r \geq 0 \tag{5.5}$$

The complex envelope for both Rician and Rayleigh can be given by h = I + jQ. Here, the channel coherence time exceeds the observation time hence slow fading is considered. This implies that the channel response remains constant for all transmitted signal x(t). The impulse response is given by

$$h = P_{\text{LOS}} + \frac{1}{\sqrt{2d^\alpha}} * (randn(1,1) + 1j * randn(1,1)) \tag{5.6}$$

where

- α is the loss exponent

- d is the distance between the transmitter and the receiver

- P_{LOS} is the power of the direct LOS path

When P_{LOS} is zero, we get

$$h = \frac{1}{\sqrt{2d^\alpha}} * (randn(1,1) + 1j * randn(1,1)) \tag{5.7}$$

The transmitted signal after modulation is given as

$$x(t) = Re\{x(t)e^{j(2\pi f_c t)}\} \tag{5.8}$$

where f_c is the carrier frequency. Depending on the switching algorithm, it is set as mmWave or microwave. The received signal consists of scaled and delayed versions of the transmitted signal.

Pulse shaping is applied by interpolating the signal using a raised cosine filter. The built-in functions *RaisedCosineTransmitFilter* and *RaisedCosineReceiveFilter* of MATLAB are used for the same. The filter shape is defined as a square root. The number of symbols the filter spans is defined as 10. The ideal raised cosine filter has an infinite impulse response so the impulse response is truncated to the value specified in *FilterSpanInSymbols*. The raised cosine filter has unit energy and applies the linear gain to obtain final tap values. The number of taps of the filter is given by Equation 5.9. The specifications of the filter are mentioned in Table 5.2.

$$Taps = (FilterSpanInSymbols * OutputSamplesPerSymbol) + 1 \tag{5.9}$$

The roll-off factor is a measure of the excess bandwidth of the filter, i.e., the bandwidth occupied beyond the Nyquist bandwidth of $1/2T$, where $1/T$ is the symbol rate. Hence, the roll-off factor should be small for bandwidth efficiency.

Parameters	Values
Roll-off factor	0.5
FilterSpanInSymbols	10
OutputSamplesPerSymbol	8
Gain	1

Table 5.2 – Specifications of Root Raised Cosine Filter

For the second setup with multiple nodes, same channel model is considered for each link. The links between the transmitter and the receivers are treated independently i.e., the obstacle in one link does not necessarily imply that the neighbouring link is also blocked. An OFDM 2X2 MIMO system is used for each link.

5.2   Results

I have implemented two cases when switching from mmWave to microwave frequencies.
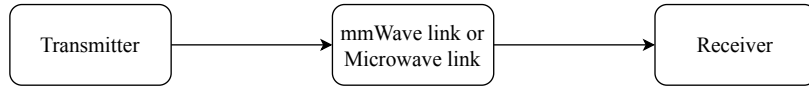
Figure 5.1 – Case 1 (Old model): Carrier frequency is generated based on the switching algorithm. There is no permanent communication link between transmitter and receiver.
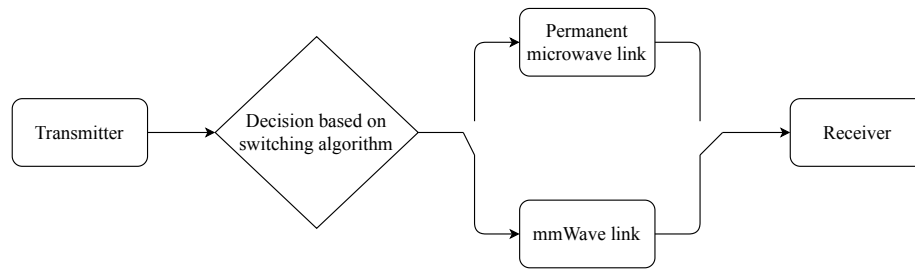
Figure 5.2 – Case 2: A permanent microwave link is present between the transmitter and the receiver.

- Case 1: The carrier frequency is generated depending on the decision of the switching algorithm and then the transmission takes place. This case has been referred to as 'Old Model' further in the thesis. This model is shown in Figure 5.1.

- Case 2: A permanent microwave link is available and the generation of the carrier frequency is not required each time. If the direct path is not available, the transmission switches to the permanent microwave link. This model is shown in Figure 5.2.

I have done a comparison study between the two cases based on the worst-case *switching time* and the channel usage. *Switching time* is defined as the period starting from the instant when the test signal is sent to the receiver when checking for LOS availability to the instant when the actual transmission starts.
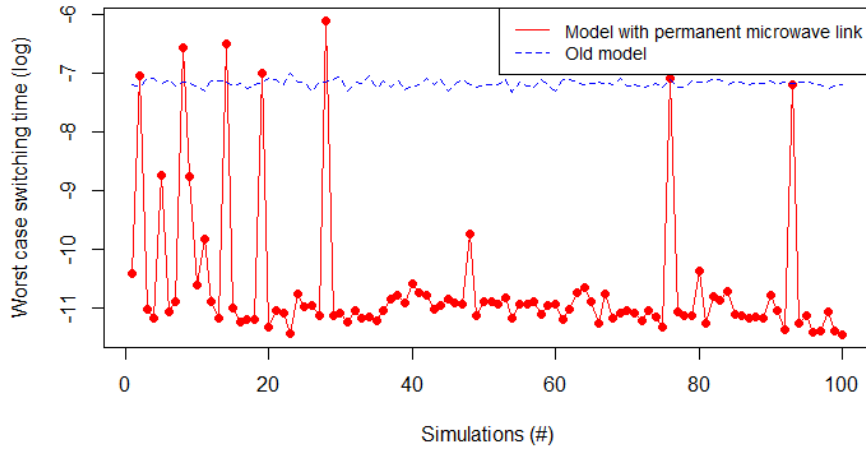
Figure 5.3 – Comparison of worst case switching time for the two models implemented for the switching algorithm.

Figure 5.3 shows a comparison based on the worst-case *switching time* of both the cases. I have executed a total of 100 simulation runs for both the cases and recorded the worst value of the *switching time*. Since the values of time were really small, I have used a log scale to make the graph more readable. Case 2 i.e., the model with permanent microwave link performs better in almost 90% of the cases. It is interesting to note that there are a few peaks in the graph. These peaks correspond to those cases where the switching algorithm has to wait until the results of the second step of LOS path check are completed. These simulations take more time to switch to the desired frequency before beginning the transmissions.

I have also compared the two cases on based on the channel used during the simulation runs. Percentage of channel usage for both cases have been plotted. Figure 5.4 shows that the model with permanent microwave link uses the microwave link for the whole duration of simulation i.e., 100% usage. Although the microwave link is not being used for the entire duration, it still has to be kept available for use.
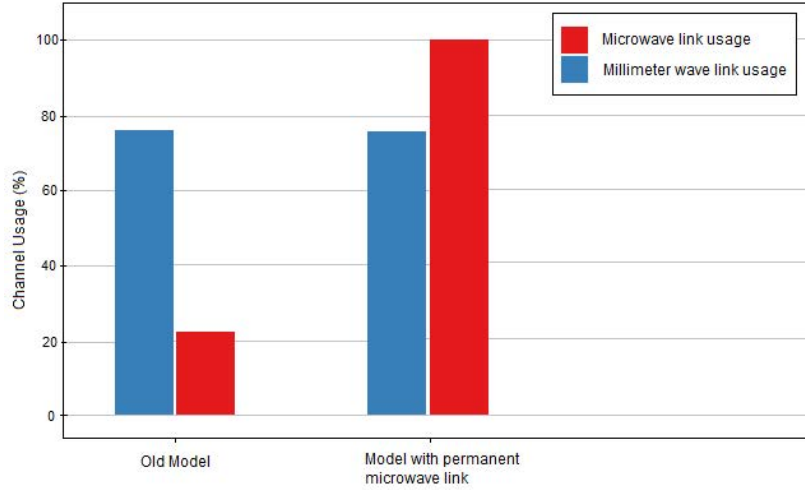
Figure 5.4 – Comparison of channel usage for the two models implemented for the switching algorithm. The first model switches the carrier frequency based on the decision of the LOS check (referred to as Old Model). The second model has a permanent microwave link which remains available throughout the duration of the simulation. Depending the decision of the LOS a switch is made from mmWave link to microwave link or vice versa.

This is disadvantageous for other users who try to access the microwave channel for other use.

Both cases have their advantages and disadvantages. When using mmWave higher data rates and faster transmissions are important factors. Hence, the second model has been used further in the thesis because of its better performance in terms of *switching time*.

The evaluation of the proposed scheduling algorithm is done by comparing the fault tolerant version of mmWave with the non fault-tolerant version. This comparison is done based on mean throughput and maximum end-to-end latency. Figures 5.5 and 5.6 show the two comparisons respectively.

The plot in Figure 5.5 shows that the fault-tolerant mmWave has the best mean throughput as compared to microwave and simple mmWave links. In case of blocked LOS, the simple mmWave has zero transmission whereas the fault-tolerant mmWave can switch to microwave and continue transmitting and does not waste time. The bandwidth is decreased since when the transmission is switched to microwave frequency. The *switching time* is quite small as compared to the transmission time and hence does not have a major affect on the throughput. The transmission done only using microwave link has less attenuation due to blockages as compared to the mmWave. It has the least throughput because of lesser bandwidth.
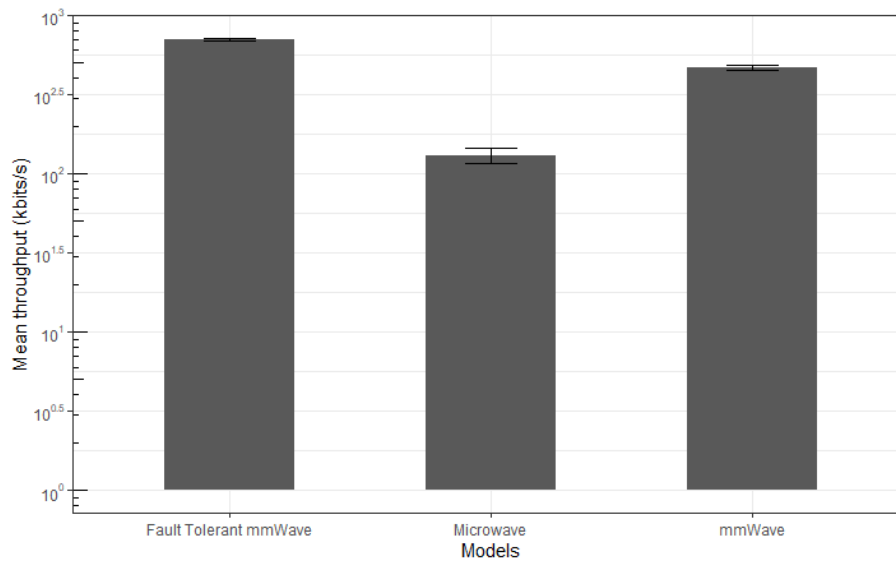
Figure 5.5 – Comparison of mean throughput for fault-tolerant mmWave, mmWave and microwave. The plot includes 95% confidence intervals for the mean values over all runs.
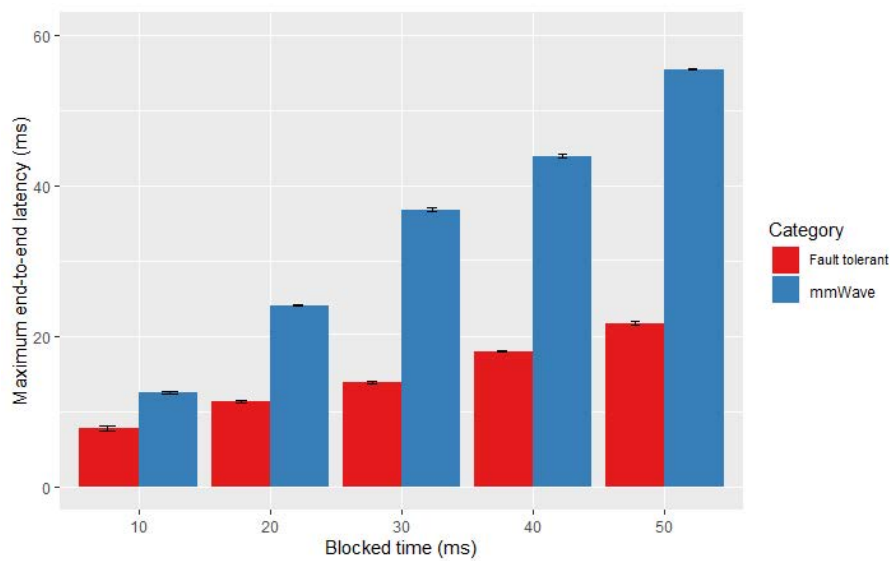

Figure 5.6 – Comparison of maximum end-to-end latency of fault tolerant mmWave and mmWave. The plot includes 95% confidence intervals for the mean values over all runs.

Figure 5.6 compares the maximum end-to-end latency of the fault-tolerant mmWave with that of mmWave. The end-to-end latency has been plotted against the *blocked time*. *Blocked time* is the total time when the LOS is blocked. The maximum latency of the mmWave increases as the blocked time increases because the

transmitted packet is lost when there is an obstacle in the direct path. A successful transmission can only take place when there is LOS between the transmitter and the receiver. In the case of fault-tolerant mmWave the blocked time does not have a major negative impact on the latency. The time taken to switch to microwave frequency gets added to the latency but it is very small compared to the total blocked time. Hence, the fault-tolerant mmWave has much smaller end-to-end latency.

5.2.1 Channel Estimation

A further extension was the system was implemented using OFDM MIMO system. Channel estimation can be done using LS estimator or MMSE. Both the estimators were simulated to decide which performed better in terms of BER. A comparison was done by plotting BER vs SNR graph which is shown in Figure 5.7. From the plot, we can see that the MMSE estimator has a better performance. MMSE has a higher complexity but has lower BER values for higher SNR.
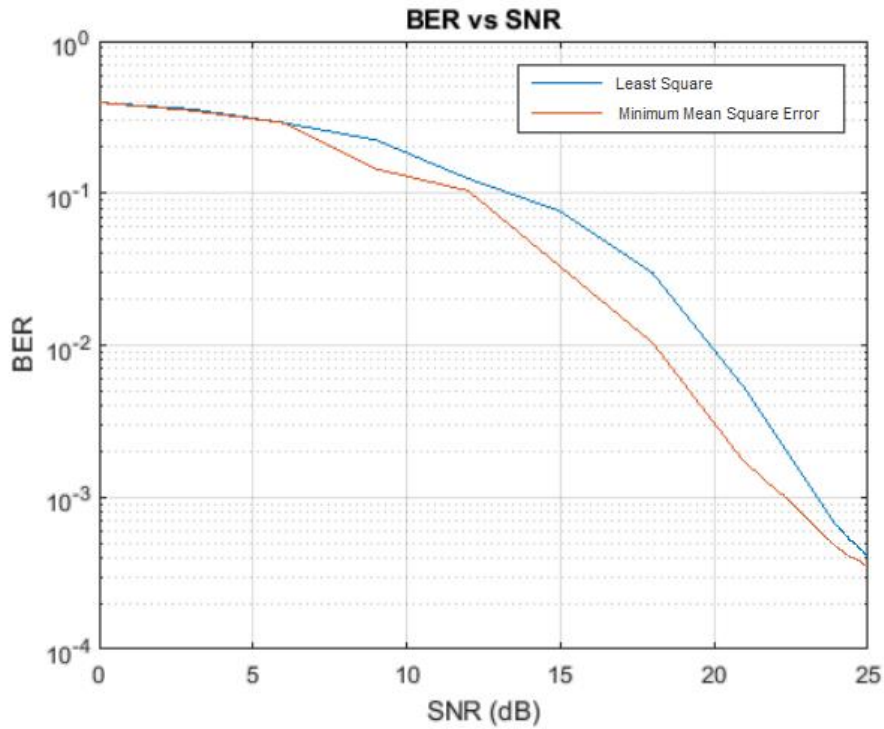
Figure 5.7 – Comparison between LS and MMSE estimators on the basis of BER vs SNR

Comparison of the estimated channel with the theoretical channel (referred to as 'true channel') in terms of power at each sub-carrier index can help in determining the performance of the estimators. The pilot sub-carriers must be interpolated for

estimating the channel for data symbols. Two types of interpolations are used with LS and MMSE estimators. These are linear and spline interpolations. DFT technique as mentioned in Section 3.4 is also applied to improve the performance of the estimators. A comparison of the following estimators is done by plotting the power of the channel vs the subcarrier index of the channel [38].

- LS estimator

  - Linear interpolation with and without DFT
  - Spline interpolation with and without DFT

- MMSE estimator with and without DFT
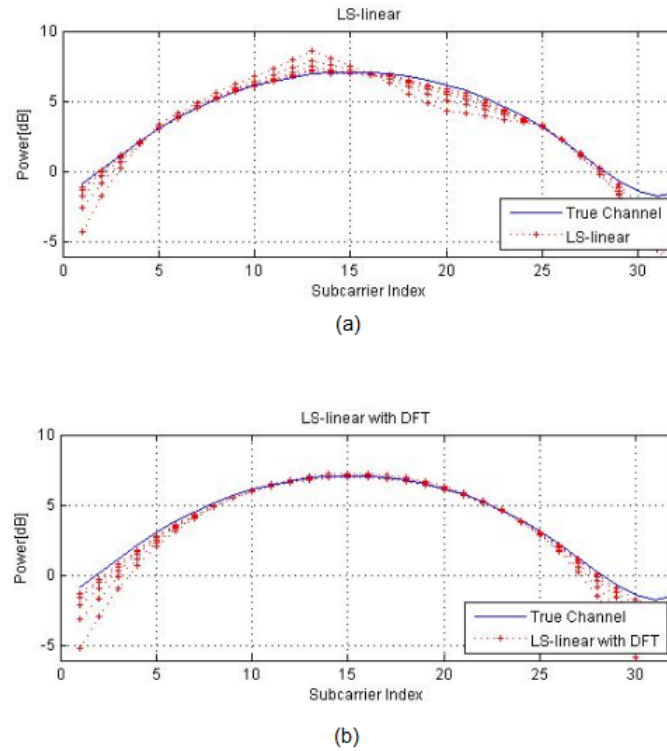
Figure 5.8 – Comparison of linear interpolation LS estimator (a) without DFT and (b) with DFT [38]

Figure 5.8 shows a comparison between linear interpolation LS estimator with and without DFT. The LS estimator with DFT gives a good estimate of the power of the true channel with little variations. The LS estimator without DFT also accounts for the noise outside the maximum delay of the channel and hence has major deviations from the true channel.
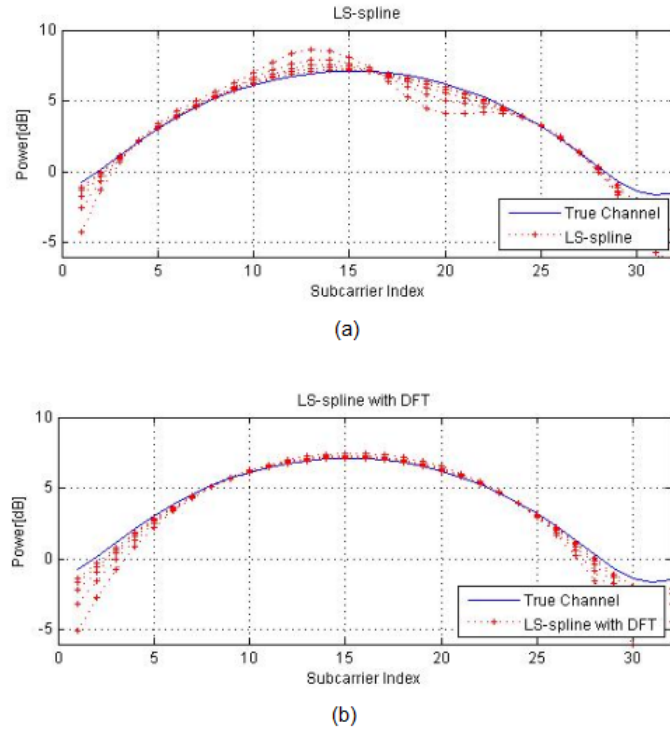
**Figure 5.9** – Comparison of spline interpolation LS estimator (a) without DFT and (b) with DFT [38]

Figure 5.9 shows a comparison between spline interpolation LS estimator with and without DFT technique. A similar behaviour is seen for LS estimator using spline interpolation. Estimator with DFT performs better in the case of spline interpolation.

Figure 5.10 shows MMSE estimators with and without DFT technique. The MMSE estimators show a better performance as compared to LS estimators. Although MMSE estimators have a higher complexity, they give a better estimate of the channel.

Using MMSE estimator, the channel estimate was calculated between the transmitter and the receivers. For comparing the results of channel estimation based switching with the previously implemented switching algorithm, I have used the metric end-to-end latency. Figure 5.11 shows a comparison between fault-tolerant mmWave and fault-tolerant mmWave with channel estimation. The maximum end-to-end latency for the fallback mechanism with channel estimation is lower than that for fault tolerant mmWave.The reason for the improvement is that with channel estimation the LOS check is not done after transmitting each packet. This reduces the delay which is introduced because of the two-step check done for confirming LOS. Introducing channel estimation and OFDM increases the complexity of the system, but it helps in exploiting the time and frequency correlation of the channel.

(a)

(b)
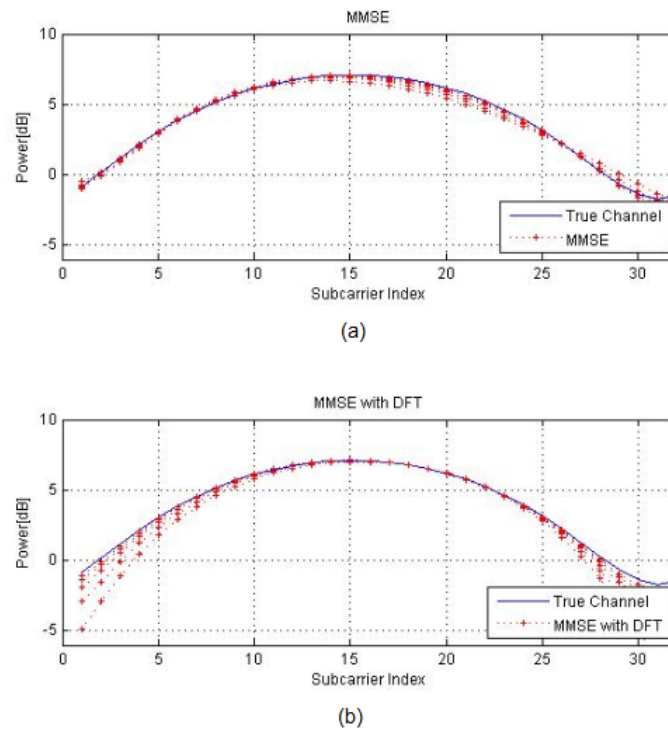
Figure 5.10 – Comparison of MMSE estimator (a) without DFT and (b) with DFT [38]
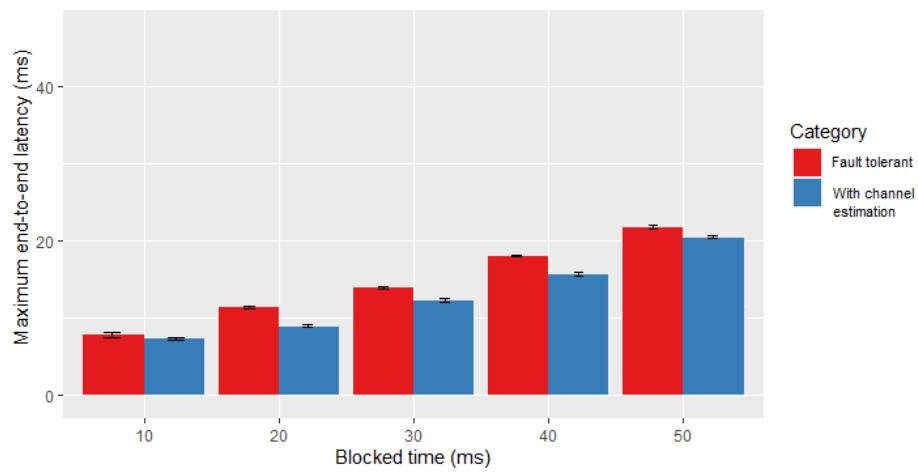
Figure 5.11 – Comparison of maximum end-to-end latency of fault-tolerant millimeter wave with and without channel estimation technique. The plot includes 99% confidence interval over all simulation runs.

This in turn reduces the latency and thereby improving the fallback mechanism of the mmWave.

Chapter 6

Conclusion

In this thesis, I have proposed a radio fallback mechanism for mmWave link. For this purpose, I have devised a switching algorithm to be used when switching from mmWave to a microwave frequency. I have used this algorithm in two cases and analysed the results from both the cases. Additionally, I have used a channel estimation technique to extend the radio fallback mechanism for multiple receivers. To analyse the various mechanisms, I ran simulations to record parameters which help in identifying the advantages and disadvantages of the mechanisms.

The results show that mmWave with radio fallback can provide better throughput as compared to the non fault tolerant mmWave. In case of blocked LOS path, fault-tolerant mmWave has less end-to-end latency as compared to simple mmWave. The switching algorithm was implemented for two cases. The results show that both cases have their advantages and disadvantages. The model with permanent microwave link performs well in terms of time whereas the other model has a better channel utilisation. When the system is extended for multiple receivers, fault tolerant mmWave with channel estimation proved to be better in terms of latency as compared to the fault tolerant mmWave with only switching mechanism. These results indicate that millimeter wave with radio fallback has better throughput and lower latency than mmWave.

6.1   Future Work

Although the results of this thesis show evident advantages, it is possible to further improve the fallback mechanism. Piggybacking can be used to further reduce latency. Piggybacking would also aid preemptive scheduling of the microwave link instead of having a permanent link. Furthermore, the channel estimation technique used in this thesis employs 2X2 MIMO system. It would be interesting to see if having more than 2 transmitter and receiver antennas would further improve the system.

The simple algorithm I have used in the implementation already shows promising results. Based on these, more sophisticated algorithms can be developed, such as e.g., adaptive thresholding. The current algorithm uses hard thresholds for determining the state of LOS link. This algorithm can be further improved so that it can be used with all kinds of channel models without having to change the thresholds.

List of Abbreviations

3GPP	3rd Generation Partnership Project
AWGN	Additive White Gaussian Noise
BER	Bit Error Rate
BPSK	Binary Phase Shift Keying
D2D	Device-to-Device
DFT	Discrete Fourier Transform
FFT	Fast Fourier Transform
FSPL	Free Space Path Loss
HD	High Definition
IFFT	Inverse Fast Fourier Transform
ISI	Inter Symbol Interference
LMMSE	Linear Minimum Mean-Square Error
LOS	Line of Sight
LS	Least Square
MIMO	Multiple Input Multiple Output
MMSE	Minimum Mean-Square Error
mmWave	Millimeter Wave
nLOS	non Line of Sight
OFDM	Orthogonal Frequency Division Multiplexing
PDF	Probability Density Function
QPSK	Quadrature Phase Shift Keying
rms	root mean square
RRC	Root Raised Cosine
SISO	Single Input Single Output
SNR	Signal-to-Noise Ratio
VLC	Visible Light for Communication
WiGig	Wireless Gigabit

List of Figures

List of Tables

Bibliography

[1]   T. S. Rappaport, J. N. Murdock, and F. Gutierrez, "State of the Art in 60-GHz Integrated Circuits and Systems for Wireless Communications," *Proceedings of the IEEE*, pp. 1390–1436, Jul. 2011. DOI: `10.1109/JPROC.2011.2143650`.

[2]   X. Wang, L. Kong, F. Kong, F. Qiu, M. Xia, S. Arnon, and G. Chen, "Millimeter Wave Communication: A Comprehensive Survey," *IEEE Communications Surveys Tutorials*, vol. 20, no. 3, pp. 1616–1653, 2018. DOI: `10.1109/COMST.2018.2844322`.

[3]   T. S. Rappaport, S. Sun, R. Mayzus, H. Zhao, Y. Azar, K. Wang, G. N. Wong, J. K. Schulz, M. Samimi, and F. Gutierrez, "Millimeter Wave Mobile Communications for 5G Cellular: It Will Work!" *IEEE Access*, pp. 335–349, May 2013. DOI: `10.1109/ACCESS.2013.2260813`.

[4]   P.-H. Kuo and A. Mourad, "Millimeter wave for 5G mobile fronthaul and backhaul," in *European Conference on Networks and Communications (EuCNC)*, Oulu, Finland, Jun. 2017, pp. 1–5. DOI: `10.1109/EuCNC.2017.7980750`.

[5]   I. A. Hemadeh, K. Satyanarayana, M. El-Hajjar, and L. Hanzo, "Millimeter-Wave Communications: Physical Channel Models, Design Considerations, Antenna Constructions, and Link-Budget," *IEEE Communications Surveys & Tutorials*, vol. 20, no. 2, pp. 870–913, 2017. DOI: `10.1109/COMST.2017.2783541`.

[6]   M. Shafi, J. Zhang, H. Tataria, A. F. Molisch, S. Sun, T. S. Rappaport, F. Tufvesson, S. Wu, and K. Kitao, "Microwave vs. Millimeter-Wave Propagation Channels: Key Differences and Impact on 5G Cellular Systems," *IEEE Communications Magazine (COMMAG)*, vol. 56, no. 12, pp. 14–20, Dec. 2018. DOI: `10.1109/MCOM.2018.1800255`.

[7]   H. Shokri-Ghadikolaei, C. Fischione, G. Fodor, P. Popovski, and M. Zorzi, "Millimeter Wave Cellular Networks: A MAC Layer Perspective," *IEEE Transactions on Communications*, vol. 63, no. 10, pp. 3437–3458, Oct. 2015. DOI: `10.1109/TCOMM.2015.2456093`.

[8] Y. Niu, Y. Li, D. Jin, L. Su, and A. V. Vasilakos, "A survey of millimeter wave communications (mmWave) for 5G: opportunities and challenges," *Wireless Networks*, vol. 21, no. 8, pp. 2657–2676, Nov. 2015. DOI: 10.1007/s11276-015-0942-z.

[9] R. Congiu, H. Shokri-Ghadikolaei, C. Fischione, and F. Santucci, "On the relay-fallback tradeoff in millimeter wave wireless system," in *2016 IEEE Conference on Computer Communications Workshops (INFOCOM WKSHPS)*, San Francisco, CA, Apr. 2016, pp. 622–627. DOI: 10.1109/INFCOMW.2016.7562151.

[10] L. Kong, L. Ye, F. Wu, M. Tao, G. Chen, and A. V. Vasilakos, "Autonomous Relay for Millimeter-Wave Wireless Communications," *IEEE Journal on Selected Areas in Communications (JSAC)*, vol. 35, no. 9, pp. 2127–2136, Sep. 2017. DOI: 10.1109/JSAC.2017.2720518.

[11] S. Biswas, S. Vuppala, J. Xue, and T. Ratnarajah, "On the Performance of Relay Aided Millimeter Wave Networks," *IEEE Journal of Selected Topics in Signal Processing*, vol. 10, no. 3, pp. 576–588, 2016. DOI: 10.1109/JSTSP.2015.2509951.

[12] F. Wang, H. Wang, H. Feng, and X. Xu, "A Hybrid Communication Model of Millimeter Wave and Microwave in D2D Network," in *83rd IEEE Vehicular Technology Conference (VTC Spring)*, Nanjing, China, May 2016, pp. 1–5. DOI: 10.1109/VTCSpring.2016.7504074.

[13] O. Semiari, W. Saad, M. Bennis, and M. Debbah, "Integrated Millimeter Wave and Sub-6 GHz Wireless Networks: A Roadmap for Joint Mobile Broadband and Ultra-Reliable Low-Latency Communications," *IEEE Transactions on Wireless Communications (TWC)*, vol. 26, no. 2, pp. 109–115, 2019. DOI: 10.1109/MWC.2019.1800039.

[14] M. Alrabeiah and A. Alkhateeb, "Deep Learning for mmWave Beam and Blockage Prediction Using Sub-6 GHz Channels," *IEEE Transactions on Communications*, vol. 68, no. 9, pp. 5504–5518, 2020. DOI: 10.1109/TCOMM.2020.3003670.

[15] H. He, C.-K. Wen, S. Jin, and G. Y. Li, "Deep Learning-Based Channel Estimation for Beamspace mmWave Massive MIMO Systems," *IEEE Wireless Communications Letters*, vol. 7, no. 5, pp. 852–855, 2018. DOI: 10.1109/LWC.2018.2832128.

[16] X. Cheng, C. Tang, and Z. Zhang, "Accurate Channel Estimation for Millimeter-Wave MIMO Systems," *IEEE Transactions on Vehicular Technology (TVT)*, vol. 68, no. 5, pp. 5159–5163, May 2019. DOI: 10.1109/TVT.2019.2905640.

[17] X. Zhu, A. Doufexi, and T. Kocak, "Throughput and Coverage Performance for IEEE 802.11ad Millimeter-Wave WPANs," in *73rd IEEE Vehicular Technology Conference (VTC Spring)*, Yokohama, Japan, May 2011, pp. 1–5. DOI: 10.1109/VETECS.2011.5956194.

[18] A. K. Gupta, J. G. Andrews, and R. W. Heath, "Impact of Correlation between Link Blockages on Macro-Diversity Gains in mmWave Networks," in *2018 IEEE International Conference on Communications Workshops (ICC Workshops)*, Kansas City, MO, May 2018, pp. 1–6. DOI: 10.1109/ICCW.2018.8403598.

[19] Q. C. Li, G. Wu, and T. S. Rappaport, "Channel model for millimeter-wave communications based on geometry statistics," in *2014 IEEE Globecom Workshops (GC Wkshps)*, Austin, TX, Dec. 2014, pp. 427–432. DOI: 10.1109/GLOCOMW.2014.7063469.

[20] M. R. Akdeniz, Y. Liu, M. K. Samimi, S. Sun, S. Rangan, T. S. Rappaport, and E. Erkip, "Millimeter Wave Channel Modeling and Cellular Capacity Evaluation," *IEEE Journal on Selected Areas in Communications (JSAC)*, vol. 32, no. 6, pp. 1164–1179, Jun. 2014. DOI: 10.1109/JSAC.2014.2328154.

[21] H. Shokri-Ghadikolaei and C. Fischione, "The Transitional Behavior of Interference in Millimeter Wave Networks and Its Impact on Medium Access Control," *IEEE Transactions on Communications*, vol. 64, no. 2, pp. 723–740, Feb. 2016. DOI: 10.1109/TCOMM.2015.2509073.

[22] Z. Pi and F. Khan, "An introduction to millimeter-wave mobile broadband systems," *IEEE Communications Magazine (COMMAG)*, vol. 49, no. 6, pp. 101–107, 2011. DOI: 10.1109/MCOM.2011.5783993.

[23] O. E. Ayach, S. Rajagopal, S. Abu-Surra, Z. Pi, and R. W. Heath, "Spatially Sparse Precoding in Millimeter Wave MIMO Systems," *IEEE Transactions on Wireless Communications (TWC)*, vol. 13, no. 3, pp. 1499–1513, 2014. DOI: 10.1109/TWC.2014.011714.130846.

[24] H. Shokri-Ghadikolaei, F. Boccardi, C. Fischione, G. Fodor, and M. Zorzi, "Spectrum Sharing in mmWave Cellular Networks via Cell Association, Coordination, and Beamforming," *IEEE Journal on Selected Areas in Communications*, vol. abs/1605.05578, Nov. 2016. DOI: 10.1109/JSAC.2016.2615259.

[25] M. Xiao, S. Mumtaz, Y. Huang, L. Dai, Y. Li, M. Matthaiou, G. K. Karagiannidis, E. Björnson, K. Yang, C.-L. I, et al., "Millimeter Wave Communications for Future Mobile Networks," *IEEE Journal on Selected Areas in Communications (JSAC)*, vol. 35, no. 9, pp. 1909–1935, Sep. 2017. DOI: 10.1109/JSAC.2017.2719924.

[26] T. G. Phillips and K. B. Jefferts, "Millimeter-Wave Receivers and Their Applications in Radio Astronomy (Short Papers)," *IEEE Transactions on Microwave Theory and Techniques*, vol. 22, no. 12, pp. 1290–1292, 1974. DOI: `10.1109/TMTT.1974.1128479`.

[27] M. Choi, G. Lee, S. Jin, J. Koo, B. Kim, and S. Choi, "Link Adaptation for High-Quality Uncompressed Video Streaming in 60-GHz Wireless Networks," *IEEE Transactions on Multimedia*, vol. 18, no. 4, pp. 627–642, Apr. 2016. DOI: `10.1109/TMM.2016.2525012`.

[28] R. Appleby and R. N. Anderton, "Millimeter-Wave and Submillimeter-Wave Imaging for Security and Surveillance," *Proceedings of the IEEE*, vol. 95, no. 8, pp. 1683–1690, Aug. 2007. DOI: `10.1109/JPROC.2007.898832`.

[29] D. Sheen, D. Mcmakin, and T. Hall, "Detection of Explosives by Millimeter-wave Imaging," *Counterterrorist Detection Techniques of Explosives*, Dec. 2007. DOI: `10.1016/B978-044452204-7/50028-6`.

[30] M. Marcus and B. Pattan, "Millimeter wave propagation: spectrum management implications," *IEEE Microwave Magazine*, vol. 6, no. 2, pp. 54–62, Jun. 2005. DOI: `10.1109/MMW.2005.1491267`.

[31] B. Sklar, "Rayleigh fading channels in mobile digital communication systems. I. Characterization," *IEEE Communications Magazine (COMMAG)*, vol. 35, no. 9, pp. 136–146, Sep. 1997. DOI: `10.1109/35.620535`.

[32] R. Weiler, M. Peter, W. Keusgen, A. Maltsev, I. Karls, A. Pudeyev, I. Bolotin, I. Siaud, and A.-M. Ulmer-Moll, "Quasi-deterministic millimeter-wave channel models in MiWEBA," *EURASIP Journal on Wireless Communications and Networking*, vol. 2016, Dec. 2016. DOI: `10.1186/s13638-016-0568-6`.

[33] Y. Wang, L. Huang, Z. Shi, K. Liu, and X. Zou, "A millimeter wave channel model with variant angles under 3GPP SCM framework," in *26th IEEE Annual International Symposium on Personal, Indoor, and Mobile Radio Communications (PIMRC)*, Hong Kong, China, Aug. 2015, pp. 2249–2254. DOI: `10.1109/PIMRC.2015.7343672`.

[34] J. M. Romero-Jerez, F. J. Lopez-Martinez, J. F. Paris, and A. Goldsmith, "The Fluctuating Two-Ray Fading Model for mmWave Communications," in *2016 IEEE Globecom Workshops (GC Wkshps)*, Washington, D.C., Dec. 2016, pp. 1–6. DOI: `10.1109/GLOCOMW.2016.7849062`.

[35] A. Meijerink and A. F. Molisch, "On the Physical Interpretation of the Saleh–Valenzuela Model and the Definition of Its Power Delay Profiles," *IEEE Transactions on Antennas and Propagation*, vol. 62, no. 9, pp. 4780–4793, 2014. DOI: `10.1109/TAP.2014.2335812`.

[36] O. Edfors, M. Sandell, J.-J. van de Beek, S. K. Wilson, and P. O. Borjesson, "OFDM channel estimation by singular value decomposition," in *46th IEEE Vehicular Technology Conference (VTC)*, Atlanta, GA, Apr. 1996, 923–927 vol.2. DOI: 10.1109/VETEC.1996.501446.

[37] Y. Yang, G. Zhu, Y. Chen, and R. Tassing, "Local Linear Regression Based Channel Estimation for OFDM Systems," in *4th IEEE International Conference on Wireless Communications, Networking and Mobile Computing (WiCom 2008)*, Dalian, China, Oct. 2008, pp. 1–5. DOI: 10.1109/WiCom.2008.167.

[38] Y. S. Cho, J. Kim, W. Y. Yang, and C. G. Kang, MIMO-OFDM Wireless Communications with MATLAB. Wiley Publishing, 2010.

[39] V. B. Niranjane and D. B. Bhoyar, "Performance analysis of different channel estimation techniques," in *International Conference on Recent Trends in Information Technology (ICRTIT 2011)*, Chennai, India, Jun. 2011, pp. 74–78. DOI: 10.1109/ICRTIT.2011.5972481.

[40] R. C. Daniels and R. W. Heath, "60 GHz wireless communications: Emerging requirements and design recommendations," *IEEE Vehicular Technology Magazine (VTMag)*, vol. 2, no. 3, pp. 41–50, 2007. DOI: 10.1109/MVT.2008.915320.

[41] A. Tkac, V. Wieser, and S. Pollak, "Calculation of impulse response in Rician and Rayleigh channel," in *2012 ELEKTRO*, Rajeck Teplice, Slovakia, May 2012, pp. 99–102. DOI: 10.1109/ELEKTRO.2012.6225580.